Structural effects of interaction between lanthanum cuprate and cerium dioxide

I. E. MUKOVOZOV, A. M. EZERETS, A. V. VISHNIAKOV,
D. I. Mendeleev University of Chemical Technology of Russia, Miusskaja Sq. 9, Moscow 125190, Russia

L. FORNI*, C. OLIVA
Dipartimento di Chimica Fisica ed Elettrochimica, Universita' di Milano, via Golgi 19, 20133 Milano, Italy

In the present work the structural effects of La_2CuO_4 doping with CeO_2, or of supporting the former on the latter, have been investigated. It was found that lanthanum oxide possesses a very good solubility in cerium dioxide in the presence of copper oxide, forming a solid solution. According to our experimental data, at 1050 °C and in the presence of copper oxide (over 1.5% mass), the boundary for the existence of the $Ce_{1-z}La_zO_{2-z/2-\delta}$ phase falls between $z = 0.398$ and $z = 0.462$. Copper oxide itself has a very low, but appreciable solubility in this system. The excess of CuO strongly increases the rate of formation of the solid oxides solution, due to its relatively low melting point.

1. Introduction

During the last few years perovskite-like phases, of general formula ABO_3 and A_2BO_4, doped with various metal ions have been the subject of extensive investigations in view of their application as catalysts for deNOxing or for CO oxidation in combustion exhaust gases. One of the most explored directions is the partial substitution of A or/and B cations by ions with different radius and charge, in order to promote catalytic activity through significant distortion of the original crystal structure. It was found that either doping of a perovskite with fluorite-like oxides or supporting it on such oxides brings to a volcano-shaped raise of catalytic activity. This phenomenon was observed, for example, in the case of interaction of either ZrO_2 [1, 2] or CeO_2 [3–6] with perovskites. In such a case some interesting effects due to change of crystal properties, such as type of conductivity and oxygen non-stoichiometry, were observed. The surface properties of cerium dioxide doped with lanthanide oxides were thoroughly studied by Harrison *et al.* [7]. They concluded that calcination of lanthanide oxides with CeO_2 at elevated temperature results in segregation of the former over the surface of the latter. Thickness of the coverage increases with temperature of heat treatment. However, bulk properties of these systems have been little studied.

The scope of the present work was to investigate the possible structural effects of La_2CuO_4 doping with CeO_2, or of supporting it on the latter.

2. Experimental procedure

2.1. Preparation

Three series of samples were prepared:

Series 1: Lanthanum cuprate with partial substitution of Ce^{4+} for La^{3+} ($La_{2-x}Ce_xCuO_{4-\delta}$ $x = 0$, 0.05, 0.10, 0.15, 0.20);

Series 2: Cerium dioxide doped with lanthanum cuprate ($Ce_{1-y}La_{2y/3}Cu_{y/3}O_{2-2y/3-\delta}$, $y =$ 0.25, 0.35, 0.43, 0.50, 0.56, 0.71);

Series 3: Mixture of La_2O_3 with CeO_2 in molar ratio 1 : 2 doped with various amounts of CuO (La: Cu molar ratio being 25 : 1, 20 : 1, 15 : 1, 10 : 1, and 5 : 1).

Samples of the first two series were prepared by mixing the desired amounts of La_2O_3, CuO, and CeO_2 with ammonium nitrate. The mixture was heated slowly (2 °C min^{-1}) up to 320 °C. The oxides dissolved in melted ammonium nitrate, forming a solution of the respective nitrates. The intermediate products were then quickly heated in air up to 950 °C and kept at this temperature for 1h to decompose the nitrates. At last the samples were ground thoroughly and calcined at 1050 °C for 10 h in air.

The samples of series 3 were prepared by addition of the desired amounts of copper oxide to La_2O_3–CeO_2 mixture. Since the amount of copper oxide was very low, it was introduced by impregnating the solid mixture with an aqueous solution of $Cu(NO_3)_2$. Then the

* Author to whom any correspondence should be addressed.

0022–2461

samples were dried at 250 °C and calcined at 1100 °C for 20 h.

2.2. Sample characterization

X-ray diffraction (XRD) patterns were obtained with a Siemens D-500 diffractometer Cu$K_{\alpha 1}$-radiation. Ni-filtered) employing the Debye method and compared with literature data [8]. A Cambridge Stereoscan 150 SEM (scanning electron microscope) apparatus, coupled with a Link Mod. 860 EPMA (electron probe microanalyser) instrument, was employed to characterize the morphology and surface composition. EPMA analysis was done by integrating the counts for a preset lifetime and for a large number of different positions over the sample at various magnifications. Electron paramagnetic resonance (EPR) analysis was carried out with a Bruker EST-300 EPR-ENDOR instrument.

3. Results and discussion

XRD analysis of the first series showed that the solubility of cerium dioxide in lanthanum cuprate is very low, the upper range lying between $x = 0.00$ and $x = 0.05$. The most intense reflections present on XRD patterns (see Fig. 1) belong to lanthanum cuprate and coexist with some reflections of significantly lower intensity for $x = 0.05$–0.20 samples. The position of the last reflections was almost identical to that of pure CeO_2, but with a shift in the direction of higher values of interplanar distances d_{hkl}. We assumed that the shift is due to formation of some solid solution based on cerium dioxide.

An attempt to synthesize solid solutions of CeO_2–CuO and CeO_2–La_2O_3 at temperatures up to 1110 °C did not lead to any positive result. Even after 30 h of thermal treatment, XRD patterns contained only unshifted reflections of the precursors. So, we came to the conclusion that the formation of some

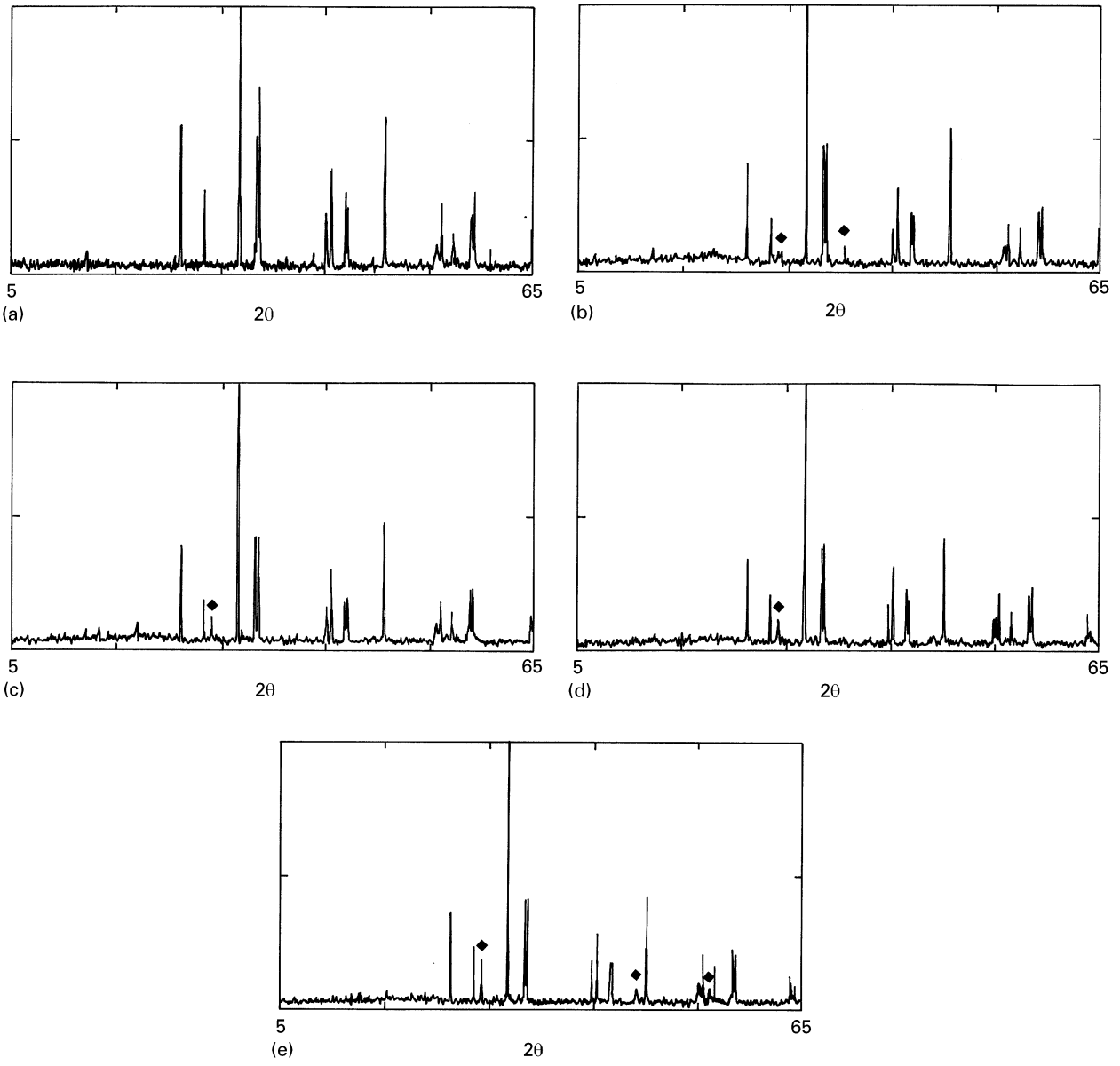

Figure 1 XRD patterns of first series $La_{2-x}Ce_xCuO_{4-\delta}$. (a) $x = 0$; (b) $x = 0.05$; (c) $x = 0.10$; (d) $x = 0.15$; (e) $x = 0.20$. (◆) Reflections of the solid solution.

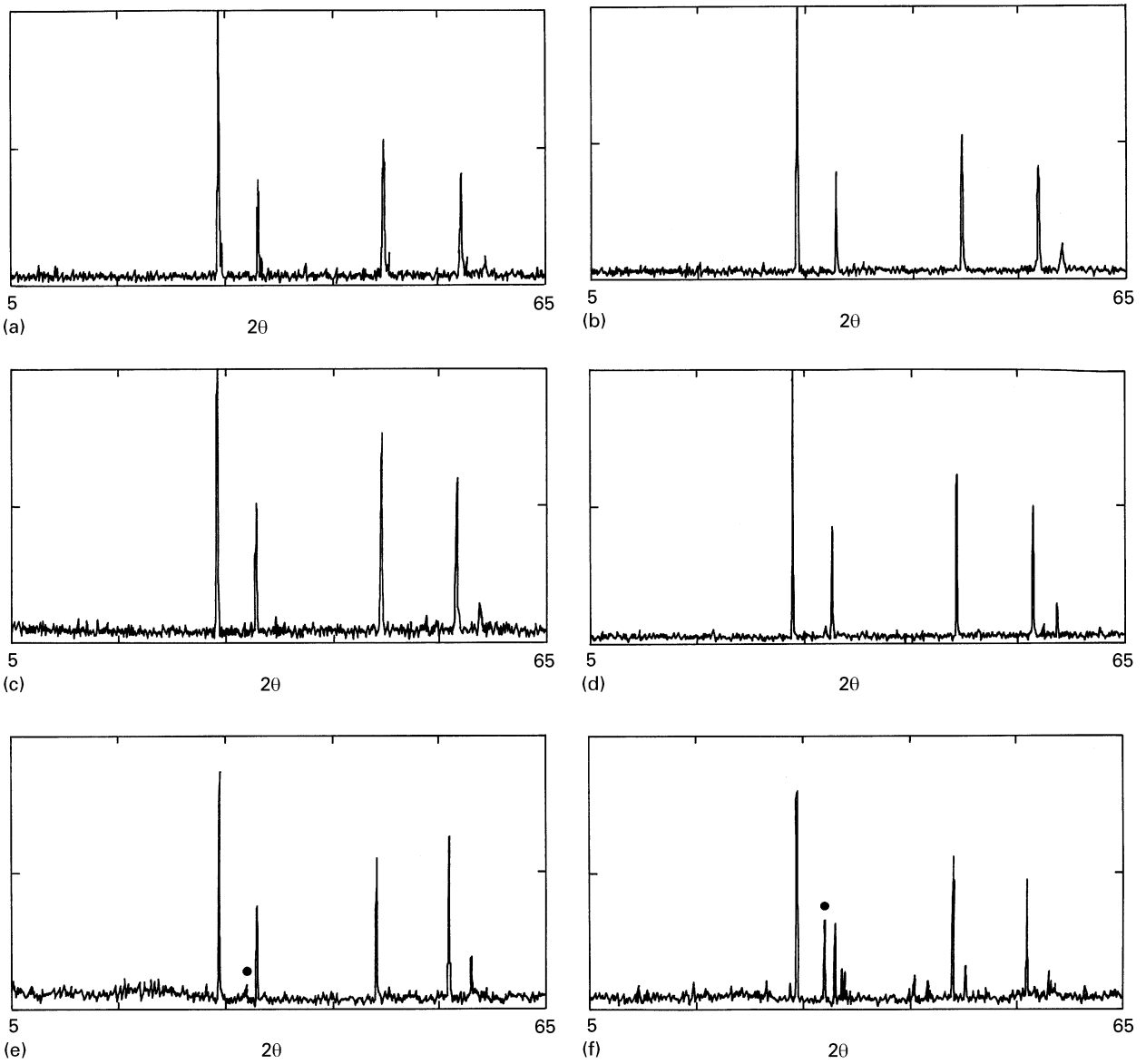

Figure 2 XRD patterns of second series $Ce_{1-y}La_{2y/3}Cu_{y/3}O_{2-2y/3-\delta}$. (a) $y = 0.25$; (b) $y = 0.35$; (c) $y = 0.43$; (d) $y = 0.50$; (e) $y = 0.56$; (f) $y = 0.71$. (●) Most intense reflections of La_2CuO_4.

solid solution based on CeO_2 at temperatures 950–1100 °C could take place only in the presence of both La_2O_3 and CuO.

The next two series were then prepared to investigate the role of the oxides in the formation of the solid solution.

The XRD patterns of the second series, of samples with $y = 0$–0.50, show only reflections, the intensity of which almost coincide with those of pure CeO_2, but their position is shifted systematically. The more pronounced the change of composition the more intense is shifting (see Fig. 2a–d). The pattern of the $y = 0.563$ sample shows also the most intense reflection of lanthanum cuprate (see Fig. 2e), but the reflections of CeO_2 do not move any further. Additional increase in y-value causes the appearance of the whole set of reflections of lanthanum cuprate with growing intensity (see Fig. 2f).

The data on interplanar distances d_{hkl} belonging to the most intense reflections of the samples are collected in Table I. The calculated lattice parameters are shown in the last column.

TABLE I Dependence of interplanar distances d_{hkl} and lattice parameter on composition for samples of series 2

		Interplanar distances, d_{hkl} (nm)				Lattice cell parameter
y	z[a]	111	200	220	311	(nm)
0.000	0.000	0.3124	0.2705	0.1913	0.1632	0.5411
0.250	0.182	0.3159	0.2737	0.1935	0.1645	0.5472
0.346	0.261	0.3171	0.2746	0.1943	0.1657	0.5495
0.429	0.334	0.3186	0.2758	0.1951	0.1664	0.5517
0.500	0.398	0.3190	0.2763	0.1955	0.1668	0.5530
0.563	0.462	0.3195	0.2767	0.1958	0.1670	0.5536
0.711	0.621	0.3194	0.2767	0.1957	0.1670	0.5537

[a] Composition of the samples recalculated according to the general formula $Ce_{1-z}La_zO_{2-z/2-\delta}$.

All the data collected in Table I refer to the temperature of synthesis (1050 °C). Thermal treatment of the saturated sample at 600 °C for 4 h did not bring any significant change in lattice parameter. This indicates a weak temperature dependence of the solubility.

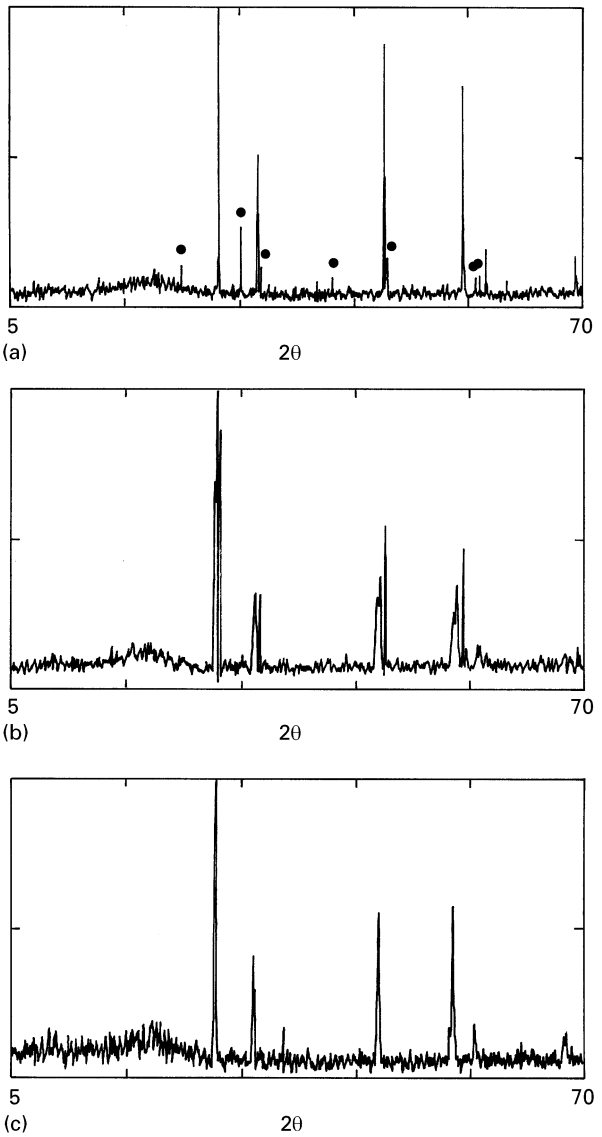

Figure 3 XRD patterns of sample 4 of second series after different time of calcination: (a) not calcined; (b) 30 min; (c) 4 h. (●) Most intense reflections of La_2CuO_4.

Therefore, in spite of the fact that neither La_2O_3 nor CuO are soluble in CeO_2 at temperatures up to 1100 °C, the calcination of the three oxides all together, as well as of the previously prepared La_2CuO_4–CeO_2, brings about the formation of a solid solution based on CeO_2. According to our experimental results, the boundary of existence of the solid solution at 1050 °C lies between $y = 0.500$ and $y = 0.563$.

The dynamics of formation of the solid solution was studied using one of the samples of series 2 ($y = 0.43$). The structure of the sample was analysed by XRD after calcination at 1050 °C for 0, 0.5, 1, 2 and 4 h (Fig. 3). After only 30 min of exposition, the reflections of lanthanum oxide, lanthanum cuprate or copper oxide could not be observed any more, while the reflections of CeO_2 became split (see Fig. 3b). Further calcination led to shift of the reflections, so that the pattern of the final sample contained only unsplit reflections of the solid solution (see Fig. 3c).

In spite of different content of lanthanum and copper oxides in cerium dioxide, which are white, black, and yellow, respectively, all the samples of series 2 had practically the same grey colour. After washing in HCl, the samples lost the grey colour and showed almost the same colour of the parent CeO_2. XRD analysis did not reveal any difference between original samples and the acid-washed ones. It is known that CuO is almost invisible by XRD in the presence of the other two oxides, due to much lower electron density. Therefore, we supposed that CuO is partially present in the system as a separate phase, deposited over the surface of the main phase, thus causing the grey colour of the samples. In order to determine the amount of separated copper oxide, the solutions obtained after washing the samples in the acid were neutralized with NH_4OH and subjected to further semiquantitative colorimetric analysis. The analysis showed that, for example for the sample $y = 0.43$, over 85% of copper oxide is not inserted in the bulk of the main phase.

The third series of samples was prepared with fixed $La_2O_3/CeO_2 = 1/2$ ratio and with increasing amounts of CuO, in order to investigate more accurately the solubility of copper oxide in the system. XRD analysis of these samples (see Fig. 4) showed a significant difference between the first three samples (La/Cu = 1/25, 1/20, and 1/15) and the last two (La/Cu = 1/10 and 1/5, respectively).

The XRD patterns of the first three samples after 20 h of thermal treatment at 1100 °C still showed the reflections of La_2O_3. The intensity of these reflections decreased from the first to the third sample. Reflections of the solid solution were significantly split. Finally, no La_2O_3 was found in the XRD patterns of samples 4 and 5, and reflections of the solid solution were unsplit, i.e. the formation of the solid solution was completed. The last patterns were identical to that of second series's sample with $y = 0.43$, possessing the same La : Ce ratio and five times as much copper. Therefore, addition of copper oxide over the amount present in sample 4 does not cause any change in XRD pattern, i.e. the composition of the solid solution remains constant. The excess of CuO, not accommodated by the bulk of the solid solution, is present in the system as a separate phase, almost invisible by XRD. As far as the concentration of copper oxide exceeds that of sample 4, it becomes sufficient to promote the formation of the solid solution under our synthesis conditions. Hence, in all the samples of the second series copper oxide is in large excess for this purpose.

The significant difference between samples 3 and 4 is outlined not only by their XRD patterns, but also by their colour, sinterization degree and EPR spectra. The colour of the first three samples was close to that of cerium dioxide. Samples 4 and 5 contained particles of two different colours: black and yellow. We suppose the former ones to belong to an excess of copper oxide, which could not be accommodated in the solid solution bulk.

The EPR patterns of samples 1–3 of the third series appeared to be almost identical to that of parent cerium dioxide (see Fig. 5a–c). The intensity of the signal slightly decreased from the first to the third sample. However, a small difference in the amount of copper oxide between sample 3 and 4 leads to an

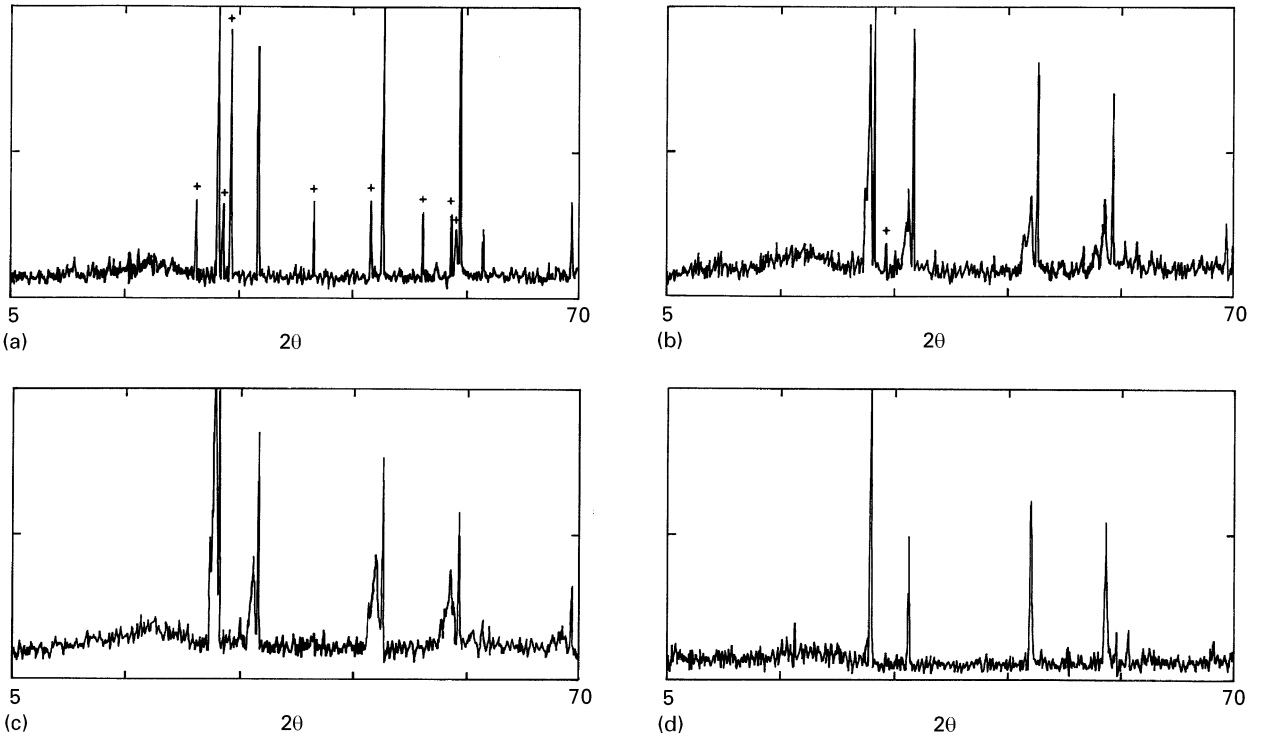

Figure 4 XRD patterns of series 3: (a) $CeO_2 + La_2O_3$ without CuO; (b) La/Cu = 25/1; (c) La/Cu = 15/1; (d) La/Cu = 10/1. (+) Most intense reflections of La_2O_3.

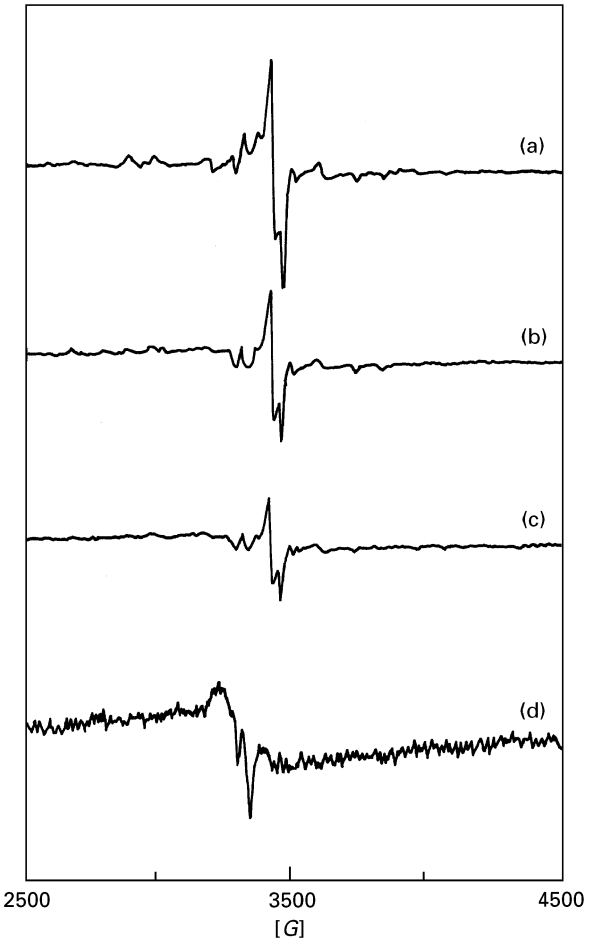

Figure 5 EPR spectra of series 3: (a) pure CeO_2; (b) La/Cu = 25/1; (c) La/Cu = 15/1; (d) La/Cu = 10/1.

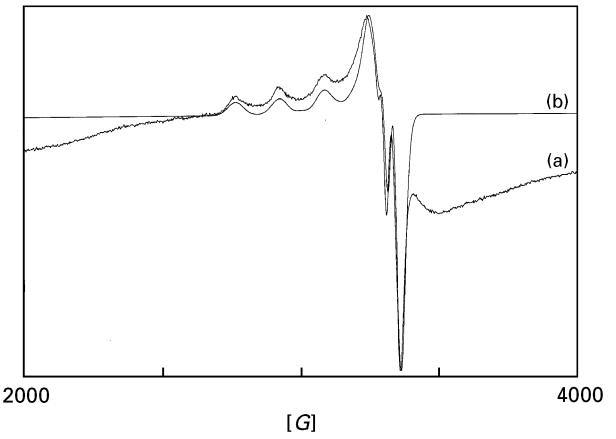

Figure 6 EPR spectra of sample 4 of series 3 at 135 K: (a) original; (b) computer-simulated.

abrupt change in the EPR signal. The original weak signal of cerium dioxide completely disappears and an EPR pattern attributable to Cu^{2+} ions is observed for both samples 4 and 5 (see Fig. 5d). For a better interpretation, sample 4 has also been analysed down to 135 K and its EPR pattern was computer-simulated with the following parameters: $g_{\parallel} = 2.238$, $g_{\perp} = 2.036$, $A_{\parallel} = 176.6$G, $A_{\perp} = 26.76$G where g is spectroscopic factor, and A is hyperfine coupling constant; G is 10^{-4}T (see Fig. 6). The spectrum perfectly overlaps those of the $y = 0.43$ sample (series 2) and of the same sample washed in HCl. Hence, the copper signal, when observed, is because of the Cu^{2+} ions inserted in the solid solution lattice, and the rest of CuO over the surface does not influence the EPR signal. The fact hat in case of samples 1–3 the last spectrum could not

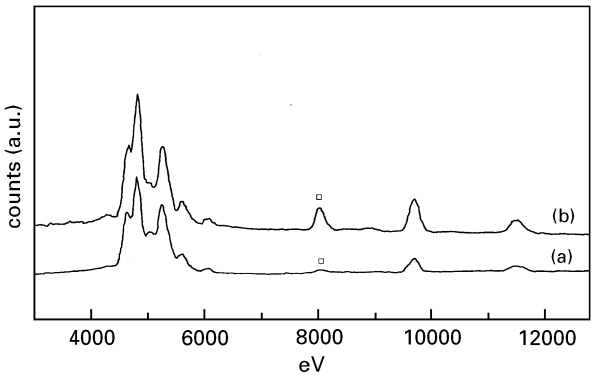

Figure 7 EPMA spectra of samples of third series, La/Cu ratio: (a) 15/1; (b) 10/1. (□) CuO characteristic peak.

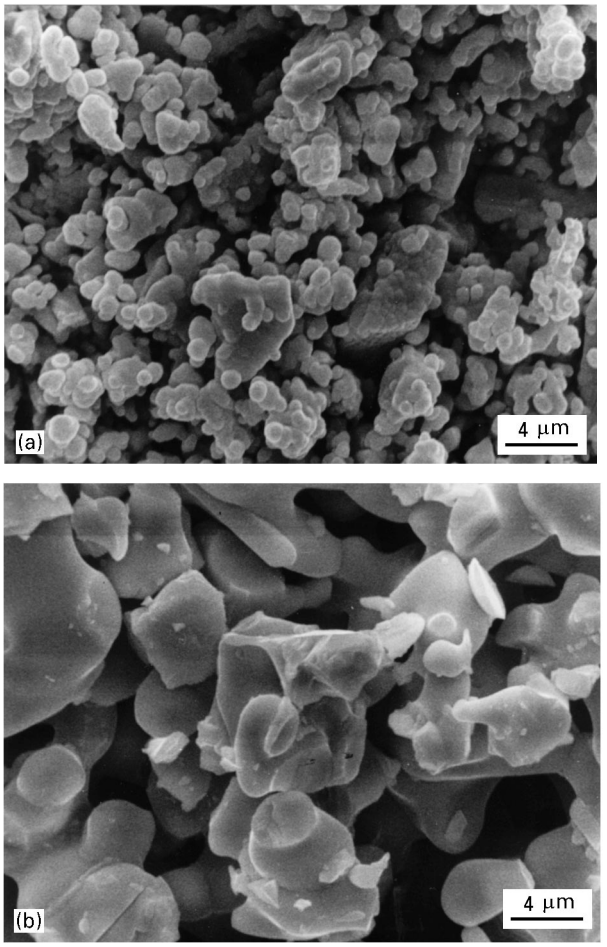

Figure 8 SEM micrographs of samples of third series, La/Cu ratio: (a) 15/1; (b) 10/1.

be observed just indicates that the formation of the solid solution is not completed.

Samples 3 and 4 of the third series were analysed also by SEM–EPMA. According to the results of EPMA analysis, surface Cu concentration (signal at ca. 8000 eV in Fig. 7a) was low for all the observed grains of sample 3. Some particles of sample 4 had practically the same copper surface concentration of sample 3. However, grains possessing at least 5–10 times higher surface copper concentration were also observed (see Fig. 7b). Microphotographs of samples surface are shown in Fig. 8. Sample 3 (Fig. 8a) appears to be unsintered, i.e. its particles are separated from

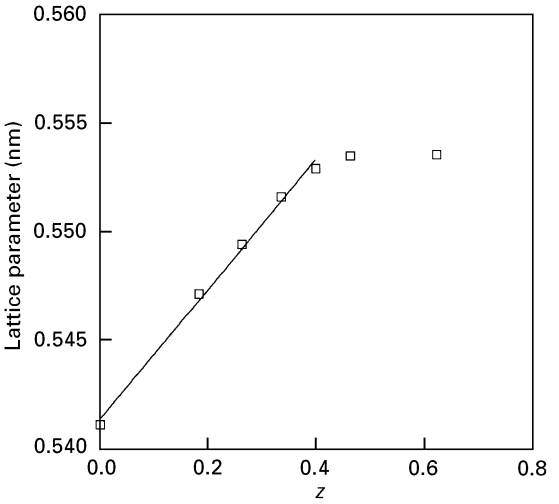

Figure 9 Range of linear dependence of lattice parameter on composition of the samples of series 2.

each other. On the opposite, sample 4 (Fig. 8b) showed a high degree of sintering. Indeed, the solid particles appear as "glued" together by thick "necks" of solid material and the size of particles is significantly larger. We attribute this high sinterization degree to the presence of an excess of CuO. This shows that sample 4 lies already in the heterogeneous region, i.e. the solubility limit for CuO falls between samples 3 and 4. Therefore, since CuO solubility in the solid solution is very low, the composition of the solution could be formally described by the general formula: $Ce_{1-z}La_zO_{2-z/2-\delta}$.

The fact that the calculated lattice parameter (see Table I) depends linearly on z-value (see Fig. 9) is in accordance with the Vègard law and consequently it can be taken as proof of the formation of the solid solution of La_2O_3 in CeO_2 in the presence of CuO.

It is of particular interest to compare our conclusions with the results reported by Harrison *et al.* [7]. According to the data of such authors, obtained through XRD and XPS (X-ray photoelectron spectroscopy) study, calcination of La_2O_3 with CeO_2 brings to the formation of lanthanum coverage over cerium surface. Those authors reported also a small shift in diffraction angles, resulting from the solid solution of the dopant in fluorite-like lattice. However, to our opinion, the change with temperature of La^{3+}/Ce^{4+} ratio on surface is not due to segregation, but just to dissolution of lanthanum oxide into the fluorite-like lattice. A significant gradient of lanthanum ions concentration through the grain of cerium oxide in our opinion indicates a low rate of the dissolution process, caused by some transport difficulties. Hence, the formation of the solid solution remains uncompleted, i.e. the system does not reach the equilibrium. Such a possibility was also considered by those authors [7]. The presence of copper oxide in our case allowed to reach the equilibrium at lower temperature and in a shorter time. We suppose CuO to play a role of flux, increasing the rate of formation of the solid oxides solution, due to its relatively low melting point.

The above results could also be compared with the data obtained by Anderson and Fierro [9] for the system La_2O_3–ZrO_2. In spite of the fact that ZrO_2 and CeO_2 possess the same fluorite-like structure,

their interaction with lanthanum oxide is of completely different type. In the former case the chemical composition $La_2Zr_2O_7$ was observed for all the samples regardless of the $La_2O_3 : ZrO_2$ ratio. On the contrary, CeO_2 does not interact chemically with La_2O_3, but forms a solid solution with a wide solubility range.

4. Conclusions

Lanthanum oxide dissolves in cerium dioxide in the presence of copper oxide, forming a solid solution. According to our data, the boundary for $Ce_{1-z}La_z$-$O_{2-z/2-\delta}$ at 1050 °C in the presence of copper oxide (over 1.5% mass) falls between $z = 0.398$ and $z = 0.462$. This means that lanthanum oxide possesses very good solubility in cerium dioxide, in spite of a significant difference in ionic radius and oxidation state.

Copper oxide itself has very low, but noticeable solubility in this system. For the Ce : La = 2 : 1 molar ratio the boundary limit rests between 2.2 and 3.2 mol %. The excess of CuO strongly increases the rate of formation of the solid solution, because of its relatively low melting point.

References

1. N. MIZUNO, *Catalysis Today* **8** (1990) 221.
2. N. MIZUNO, M. YAMATO, M. TANAKA and M. MISONO, *J. Catal.* **132** (1991) 560.
3. Y. TOKURA, H. TAKAGI and S. UCHIDA, *Nature* **337** (1989) 345.
4. G. H. KWEI, S. -W. CHEONG, Z. FISK, F. H. GARZON, J. A. GOLDSTONE and J. D. THOMPSON, *Phys. Rev.* **B40** (1989) 9370.
5. K. TABATA, I. MATSUMOTO, S. KOHIKI and M. MISONO, *J. Mater. Sci.* **22** (1987) 4031.
6. R. DOSHI, C. B. ALCOCK, N. GUNASEKARAN and J. J. CARBERRY, *J. Catal.* **140** (1993) 557.
7. P. G. HARRISON, D. A. CREASER, B. A. WOLFINDALE, K. C. WAUGH, M. A. MORRIS and W. C. MACKRODT, in "Catalysis and surface characterisation", edited by T. J. Dines, C. H. Rochester and J. T. Thomson. (The Royal Society of Chemistry, Special Publication no. 114, Cambridge, 1992) p. 76.
8. Selected powder diffraction data, Vols. 1–40. JCPDS, Swarthmore, PA, 1974–1992.
9. J. A. ANDERSON and J. L. G. FIERRO, *J. Solid State Chem.* **108** (1994) 305.

Received 17 March 1995
and accepted 18 February 1997